Role of parafacial respiratory group and active expiration on the stabilization of sleep disordered breathing

Annette Pisanski, Brianne St. Hilaire & Silvia Pagliardini
Department of Physiology, Faculty of Medicine and Dentistry, University of Alberta

UNIVERSITY OF ALBERTA

Background

It is currently hypothesized that the respiratory rhythm is generated by the interaction of two coupled oscillators in the ventral medulla: preBötzinger complex (preBötC), which generates inspiratory activity and the parafacial respiratory group (pFRG) generating active expiratory activity (mainly through the contraction of abdominal muscles, ABD) (Feldman et al. 2013) (Figure 1)

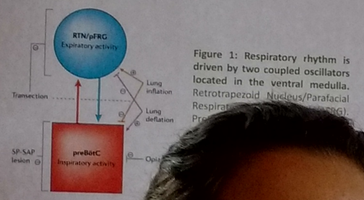

Figure 1: Respiratory rhythm is driven by two coupled oscillators located in the ventral medulla. Retrotrapezoid Nucleus/Parafacial Respirat... Pr...

Recent work in our ... expiratory ABD activ... periods of REM s... motor atonia (P... Pagliardini 2015) ... sleep, suggested ... breathing was most ... contributing to the ... events (Figure 2)

Figure ... recor...

Hypothesis

Given the association of expiratory ABD recruitment and improvement of respiratory stability in healthy sleeping rats, we hypothesize that recruitment of active expiration may occur through pFRG activation and that its occurrence stabilizes breathing and reduce SDB incidence

Methods

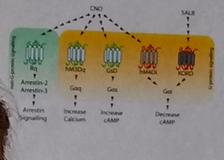

DREADDs
Designer receptor exclusively activated by designer drug

Is pFRG responsible for ABD recruitment during REM sleep?

Would excitation of pFRG help overcome sleep disordered breathing?

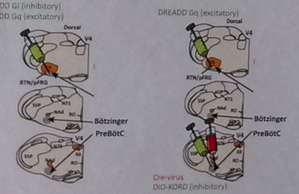

...toring of EMG and EEG activity during natural sleep ...ther vehicle or ligand systemic injections

Activation and inhibition of pFRG

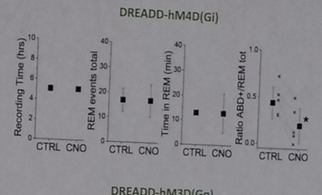

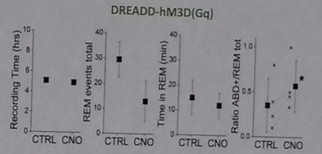

Figure 3: Inhibition and excitation of pFRG has an effect on the incidence of ABD recruitment during sleep. Top graphs: experiments performed on rats (N=5) transfected with the inhibitory DREADD Gi in control (CTRL) and after the injection of the ligand clozapine-N-oxide (CNO). Bottom graphs: experiments performed on rats (N=4) transfected with the excitatory DREADD Gq

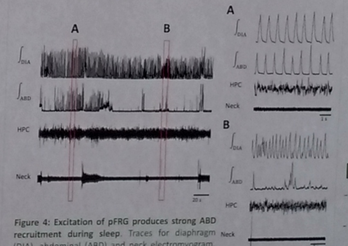

Figure 4: Excitation of pFRG produces strong ABD recruitment during sleep. Traces for diaphragm (DIA), abdominal (ABD) and neck electromyogram, as well as hippocampal (HPC) activity. Figures on the right correspond to the insets of A and B on the traces of the left

Sleep disordered breathing model

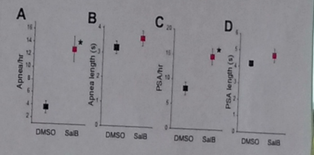

Figure 4: Inhibition of preBötC produces an increase of respiratory disturbances. Rats (N=11) were virally transfected with the inhibitory receptor KORD in the preBötC. PSA: post-sigh apnea. DMSO: dimethyl sulfoxide (vehicle). SalB: salvinorin B (KORD ligand)

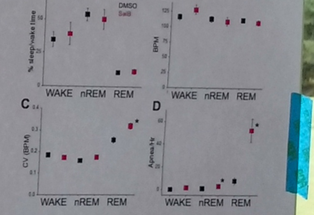

Figure 5: Respiratory disturbances occur mainly during REM sleep. BPM: breath per min. CV: coefficient of variance. DMSO: dimethyl sulfoxide (vehicle) black squares. SalB: salvinorin B (KORD ligand) red squares (N=8)

Future steps

- Complete data analysis on the sleep disordered breathing model
- Perform experiments in which we activate pFRG in the presence of a compromised preBötC

13

PHOTORECEPTOR OUTER SEGMENT LYSOSOMAL DEGRADATION DEFECTS AND IMMUNE ACTIVATION IN A MOUSE MODEL OF STGD3 MACULOPATHY

Heather Capel[1], Camille Dejos[2], Sharee Kuny[2], Yves Sauvé[1,2]
1. Department of Physiology, University of Alberta
2. Department of Ophthalmology and Visual Sciences, University of Alberta

Introduction

Stargardt-like juvenile maculopathy (STGD3) is a monogenic, early onset hereditary disorder in which photoreceptors die, causing progressive central-to-peripheral vision loss. RPE cells support photoreceptor health by phagocytosing and degrading a portion of rod outer segments each morning. Disruption of this phagocytic and lysosomal interconnection between photoreceptors and RPE in STGD3 potentially contributes to widespread damage of both cell types and eventual loss of vision.

We investigated the regulation of lysosomal degradation by Transcription Factor EB (TFEB), a key regulator of the Coordinated Lysosomal Expression and Regulation (CLEAR) gene network. TFEB nuclear translocation prior to and during peak phagocytosis was assessed, as well as gene expression of TFEB and several CLEAR genes of interest (CTSD, ATP6V0A1, and LC3). We also examined microglial cells in the eye as an indicator of immune activity.

We hypothesize that phagocytosis of POS by RPE will lead to nuclear translocation of TFEB and activation of CLEAR genes, which may be affected in STGD3 mice.

We also hypothesize that STGD3 mice will display an increased retinal microglia/macrophage population compared to WT controls, consistent with other retinal degeneration mouse models.

Methods and Materials

Tissue Collection
- Mice at 1 or 3 months
- Cull by i.P. euthanyl injection
- Look at either no light exposure or 2 hr light exposure

RPE Flat mount
- Eyes removed, fixed in 4% PFA, and cryopreserved
- 4 radial cuts to flatten eyecup
- Gently remove retina

Immunohistochemistry
- Block for 1 hr at RT
- Primary antibody overnight
- 1 hr at RT with Hoescht and secondary antibodies
- Mount with Vectashield mounting media

RNA Isolation
- Total RNA isolated from single eyecup
- Rneasy Microkit (Qiagen)
- Elute in RNAse-free water
- Quantify with Nanodrop 2000 spectrophotometer

Reverse Transcription
- Superscript III Reverse Transcription, random hexamers, RNAi
- cDNA diluted with RNAse-free water

Real-time qPCR
- SYBR Green PCR Master Mix
- Amplicon identity verified by melting curve analysis
- Target gene expression normalized to reference gene HPRT

Imaging and Analysis: Images were captured with an Olympus IX-81 inverted microscope equipped with a Hokagawa CSU X1 spinning disk confocal scan-head. Brightness and contrast levels were adjusted using ImageJ software. All analysis done in Excel.

Results

Potential defects in TFEB regulation and lysosomal pathways in STGD3

3 month: Changes in TFEB localization seen in WT flat mounts when comparing before and during phagocytosis conditions suggests change in
TFEB localization in STGD3 flat mounts does not seem different before or after phagocytosis.

1 month: More CTSD vesicle accumulation seen on apical side of RPE during phagocytosis. No increase in CTSD signal can be seen in ST
compared to WT flat mounts. Across all samples, TFEB and CTSD labeling do not colocalize.

CLEAR genes show no change in activation before or during phagocytosis

Gene expression analysis of 1 month RNA samples was done to determine quantitative changes in TFEB and three key CLEAR gen
None of the genes showed significant changes in expression, either between WT and STGD3 samples or between before and durin

Increased subretinal microglia/macrophage population seen in STGD3

Microglia-like cells were initially observed with TFEB staining of 3 month flat mounts. Iba1 labeling was used to assess the id
cells. A significantly higher number of microglia/macrophages can be seen in the subretinal space of STGD3 mice compared t

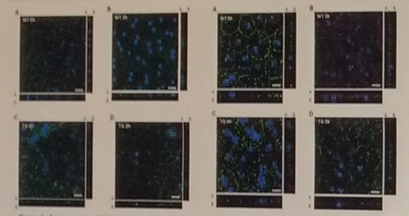

Figure 1. Representative TFEB localization in 3 month wild-type (WT) control and transgenic (TG) STGD3 mouse RPE flat mounts. TFEB labeled green, nuclei labeled blue with Hoescht staining. Apical and basal sides of orthogonal projections are labeled with "A" and "B", respectively.

Figure 2. Representative TFEB localization in 1 month wild-type (WT) control and transgenic (TG) STGD3 mouse RPE flat mounts. TFEB labeled green, CTSD labeled red, nuclei labeled blue with Hoescht staining. Apical and basal sides of orthogonal projections are labeled with "A" and "B", respectively.

Figure 3. RT-
control a
light

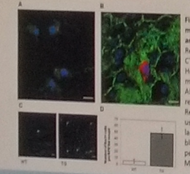

Figure 4. Immunohistochemical examination of microglia in 1 month wild-type (WT) control and transgenic (TG) STGD3 mice. A. Representative microglia. TFEB labeled green, CTSD labeled red, nuclei labeled blue with Hoescht staining. B. Determining the location of microglia within the flat mount preparation. Alexa Fluor 488 phalloidin in green, Iba1 labeled red, nuclei labeled blue with Hoescht staining. C. Representative 20x magnification field of view used for microglia/macrophage counting. Iba1 labeled green, CTSD labeled red, nuclei labeled blue with Hoescht staining. D. Counting microglia per flat mount. Results are plotted as Mean±SEM.

Futu
qPC
in t

Acknowledgements

Funding for this project provided by **Collaborative Research and Innovation Opportunities (CRIO)** grants.

Many thanks to **Dr. Camille Dejos** for her supervision and mentorship; **Sharee Kuny** for her technical knowledge and assistance; and **Dr. Yves Sauvé** for his support and supervision of this Honors Project.

Literature Cited

1. Kuny S, Gaillard E, Memo SC, et al. Inner Retina Remodeling in a Mouse Model of Stargardt-like Macular Dystrophy (STGD3). Retina. 2016;51(8):2248-2252. doi:10.1167/iovs.09-4718
2. Kuny S, Cho WJ, Dimopoulos IS, Sauvé Y. Early Onset Ultrastructure and Functional Defects in RPE and Photoreceptors of a Stargardt-Like Macular Dystrophy. *Invest Ophthalmol Vis Sci*. 2015;56(7):709-7121. doi:10.1167/iovs.15-17561
3. Settembre C, Medina DL. *TFEB and the CLEAR Network*. Vol 126. Elsevier Ltd; 2015. doi:10.1016/bs.mcb.2014.11.011.

Heather
Capel

14

1

INTRAMOLECULAR N- AND C-TERMINI INTERACTION AND PORE GATE OF TRPV1 CHANNELS

Qiaoxin Hu, Ruiqi Cai, Wang Zhang, Kong Liu, King-Zhen Chen
Membrane Protein Diseases Research Group, Department of Physiology, University of Alberta, Edmonton, AB, Canada, T6G 2H7

UNIVERSITY OF ALBERTA
EDMONTON ALBERTA-CANADA
NSERC CRSNG
CIHR IRSC

ABSTRACT

Transient receptor potential (TRP) vanilloid-1 (TRPV1) is a nonselective cation channel responding to several stimuli, including noxious heat, protons, and vanilloids. It has been well-established that TRPV1 plays essential roles in pain detection and inflammation, and has been recognized as a novel analgesic drug target. However, the molecular mechanism underlying TRPV1 gating still remains largely unclear. With mutagenesis and Xenopus oocyte electrophysiology, we identified N-terminal aromatic residue W426 and C-terminal cationic residue R701 to be critical for TRPV1 channel function. Based on the resolved TRPV1 structures showing physical proximity between the N- and C-termini, we found by co-immunoprecipitation and co-immunofluorescence that [illegible]

INTRODUCTION

The transient receptor potential vanilloid-1 (TRPV1), also known as the capsaicin receptor and the vanilloid receptor 1, is a protein encoded by the TRPV1 gene in humans. TRPV1 is a non-selective cation channel with high calcium permeability and play essential roles in pain detection and inflammation. TRPV1 can be activated by diverse stimuli, including noxious heat greater than 43 °C, protons, and vanilloids. TRPV1 is expressed in the peripheral nervous system and the central nervous system. Mutations in TRPV1 or dysregulation of TRPV1 expression have been associated to a number of human diseases, including Diabetes, Skin disorders and Bladder disorders, and TRPV1 has became an intensively pursuing target for drugs, such as analgesics.

FUNCTION OF MAMMALIAN TRPV CHANNELS

Ca²⁺ -selective channels

Non-selective Ca²⁺ permeable cation channels

TRPV1

Pain and temperature detection

TRPV2

TRPV3

Very little effect on sensory transduction, important role in skeletal, cardiac, and neuronal physiology

TRPV4

Heat activated in keratinocytes

Ca²⁺ handling in epithelial cell

TRPV5

TRPV6

RESULTS

Aromatic residue W426 and cationic residue R701 are conserved and functionally critical

TRPV1 subfamily

TRPV1 pre-S1

TRPV1 TRP domain

Rat	LLVEPSWRLLQDWDR	WKIAQEEKWKWELQHATTLYDTEKS
Mouse	LLVEPSWRLLQDWDR	WKIAQEEKWKWELQHATTLYDTEKS
Human	LLVEPSWRLLQDWDR	WKIAQEEKWKWELQHATTLYDTEKS
Chicken	LLVEPSWRLLQDWDR	WKIAQEEKWKWELQHATTLYDTEKS

Capsaicin-activated current (nA)

Fig. 1. W426 and [illegible] functionally important [illegible] summarizing averaged [illegible] from 6-9 oocytes. Cont[illegible] 2 mM KCl, 1 mM MgCl₂. [illegible] Representative immuno[illegible] membrane expression [illegible]

N- and C- terminal [illegible] length TRPV1 and [illegible]

Normalized current

Identification of gate residues in TRPV1

Hydrophobic gating

Capsaicin-activated current (nA)

Gate residue

Gate

rat TRPV1 [illegible]

[illegible] theory and TRPV1 candidate gate mutants function. A. [illegible] theory. B. Bar charts summarizing averaged capsaicin-[illegible] TRPV1 candidate gate residues, from 6-9 oocytes.

[illegible]MMARY AND CONCLUSION

[illegible]76 and C-terminal cationic residue R701 in [illegible]ction, possibly through competitive [illegible]raction.

[illegible]teraction are to be confirmed by [illegible] BPN with TRPV1-R701A and BPC [illegible] tested by experiments double [illegible]51N).

[illegible]CES

[illegible]tructure of the TRPV1 ion channel [illegible]ure. 504 (7478): 107-12. [illegible]levsky AI (2016). "Crystal structure of [illegible]n. 534 (7608): 506–11. [illegible]rophobic gating in ion channels". J Mol


12
13
PHOTORECEPTOR OUTER SEGMENT
IMMUNE ACTIVATION IN A MO
Introduction
Methods and Materials
Delineating
Absorption
YVES SAUVÉ
Heather Capel

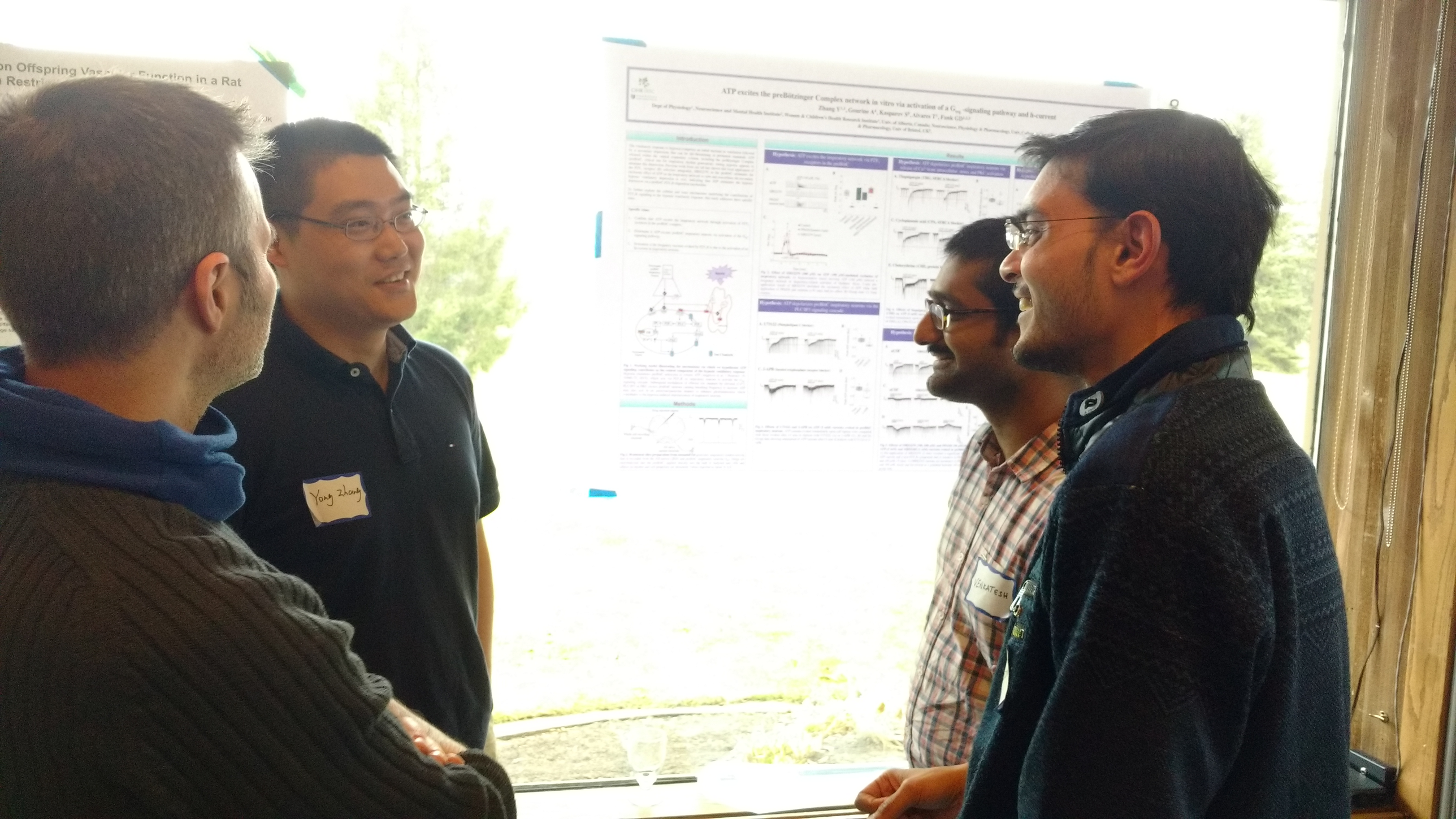
ATP excites the preBötzinger Complex network in vitro via activation of a $G_{q/11}$ signaling pathway and I$_h$-current
Introduction
Methods
Results
Hypothesis: ATP excites the inspiratory network via P2Y1 receptors in the preBötC
Hypothesis: ATP dysfunction preBötC inspiratory neurons via release of Ca2+ from intracellular stores and PKC activation
Hypothesis: ATP dysfunction preBötC inspiratory neurons via the PLC-IP3 signaling cascade
Yong Zhang
VENKATESH


Why Stem Cells & Fibrosis?
Fibrosis occurs in tissue injury
Cardiac myocardial infarction → scarring → cardiac fibrosis → heart failure → transplant/
Tissue engineering focus on cardiac tissue
Red: α-smooth muscle actin
Green: eGFP staining in infarct zone


Pro-Inflammatory Markers
Cytokine Concentration (Log) (pg/mL))
10
1
0.1
IL-6
TNFα
PBS2 Media


Katie
STARBUCKS